has been shown to be inhibited by $CaCl_2$ and KCl (4). The preparation of hydroxylamine used in CCM is hydroxylammonium hydrochloride and therefore chloride ions may be inhibiting the reaction. It may be theoretically possible to adapt the CCM method, by using another form of hydroxylamine such as hydroxylamine hydroxide, so that the OsO_4 and hydroxylamine reactions may be performed simultaneously, but this has not been investigated.

It seemed possible that the reactions could be successively performed in the same tube with a precipitation step between chemical modifications. This was tested using OsO_4 as the first chemical. The reactivity with the T mismatches varied between experiments from being not detectable to being as strong as the controls. When the osmium tetroxide was the second step, the reaction was consistently as strong as the osmium controls alone. The order of the chemicals did not affect the hydroxylamine reaction. Therefore, we suggest that the most suitable reaction condition for reliably detecting both C and T mismatches are 60 min with hydroxylamine followed by 5 min with OsO_4. The single-tube chemical cleavage of the mismatch method is given in Figure 2. This protocol is based on a recent protocol of the traditional CCM method (5). Solutions are given in other protocols (3,5).

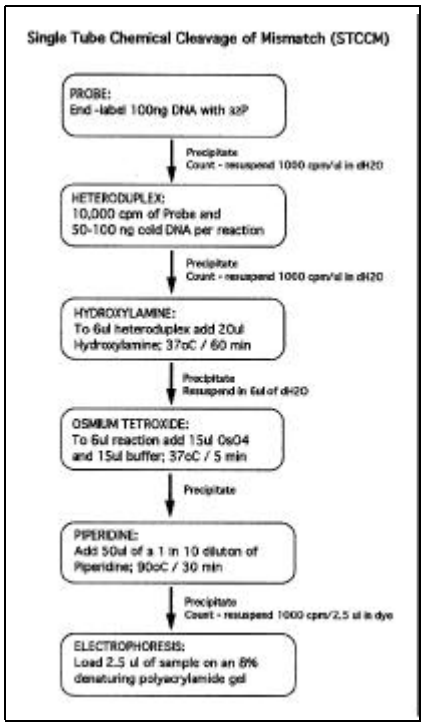

Figure 2. The single-tube chemical cleavage of mismatch method. Boxes indicated reactions, and arrows show precipitation steps. Solutions are as in the traditional CCM methods (3,5).

The use of hydroxylamine followed by OsO_4 in the same tube introduces one extra precipitation step but effectively halves the number of piperidine reactions and subsequent precipitations. As electrophoresis is required to detect mismatch bands, this change also halves the number of lanes required on an acrylamide gel. The reduction in the number of tubes and manipulations means that a single operator can screen more DNA fragments in a single day. This improvement also makes the CCM method more suitable for automation. The one minor drawback to this change is that the nature of the mismatched base is not identified. When cleavage is performed separately, a band in the hydroxylamine lane indicates a mismatched C and a band in the osmium lane a mismatched T. However, detected mismatch bands are normally sequenced to determine the actual base change. The use of the single-tube chemical cleavage of mismatch eliminates the problem of T/G mismatches, which are unreactive with osmium tetroxide (2). The C/A mismatch on the complementary heteroduplex will give a hydroxylamine reaction in the same position on the gel as the expected osmium tetroxide reaction.

REFERENCES

1. **Cotton, R.G.H.** 1993. Current methods of mutation detection. Mutat. Res. *285*:125-144.
2. **Cotton, R.G.H., H.H.M. Dahl, S. Forrest, D. Howells, S.J. Ramus, R.E. Bishop, I. Dianzani, J.A. Saleeba, E. Polombo, M.J. Anderson, C.M. Milner and R.D. Campbell.** 1993. Analysis of sequence contexts flanking T.G mismatches leads to predictions about reactivity of the mismatched T to osmium tetroxide. DNA Cell Biol. *12*:945-949.
3. **Cotton, R.G.H., N.R. Rodrigues and R.D. Campbell.** 1988. Reactivity of cytosine and thymine in single-base pair mismatches with hydroxylamine and osmium tetroxide and its application to the study of mutations. Proc. Natl. Acad. Sci. USA *85*:4397-4401.
4. **Dobi, A.L., K. Matsumoto, E. Santha and D.V. Agoston.** 1994. Guanine specific chemical sequencing of DNA by osmium tetroxide. Nucleic Acids Res. *22*:4846-4847.
5. **Ramus, S.J. and R.G.H. Cotton.** 1995. CCM: Chemical Cleavage of Mismatch, p. 50-54. Laboratory Protocols for Mutation Detection. Oxford University Press, Oxford.

Dr. Rima Youil is thanked for the DNA samples. This work was supported by a Dora Lush (Biomedical) Postgraduate Research Scholarship from the National Health and Medical Research Council of Australia. *Address correspondence to Richard Cotton, The Murdoch Institute, Royal Children's Hospital, Flemington Rd., Parkville, Victoria 3052, Australia. Internet: cotton@ cryptic.rch.unimelb.edu.au*

Received 7 July 1995; accepted 2 February 1996.

Susan J. Ramus and Richard G.H. Cotton
Royal Children's Hospital
Parkville, Victoria, Australia

Optimized Filter Set and Viewing Conditions for the S65T Mutant of GFP in Living Cells

BioTechniques 21:220-226 (August 1996)

Investigators are increasingly taking advantage of the autonomous fluorescence from the green fluorescent protein (GFP) to detect the cellular and subcellular location of GFP-fusion proteins within living cells (3,8–10,13,14). Work with these fusion constructs has shed new light on the kinetics underlying fundamental biological processes such as mitosis (9). In an attempt to study how a novel rat brain kinesin-related motor protein (rbKRP1) functions within living cells, we have transfected BHK and PC12 cells with a cDNA encoding the serine 65 → threonine 65 (S65T) GFP mutant (6) fused to the amino terminus of rbKRP1 (S65T GFP–rbKRP1). We use the S65T GFP mutant since it emits four times as

much light as the wild-type GFP (6), and it can enhance our ability to detect localized kinesin motor molecules.

Since kinesins are thought to play a role in trafficking subcellular membranous compartments along microtubules, we expected this GFP fusion construct to localize to one of the many organelles found within BHK and PC12 cells. Surprisingly, we could not determine whether the fusion construct localized, because the untransfected cells contained a large number of motile fluorescent yellow-green organelles when viewed with a standard fluorescein filter set (450–490-nm excitation filter, 510-nm dichroic beamsplitter, 515–565-nm emission filter). Untransfected and transfected cells could clearly be distinguished by eye because the GFP signal lacked the yellow tinge of the autofluorescent vesicles and had a uniform distribution within the cytoplasm. However, this color difference between the GFP signal and the autofluorescent vesicles was too subtle to determine whether there was also a punctate GFP signal. Furthermore, the punctate yellow-green fluorescent signal and the GFP signal could not be distinguished by their measured intensities in black and white digitized images acquired with a cooled charged-coupled device (CCD) camera (Photometrics, Tucson, AZ, USA).

To resolve the GFP signal from the autofluorescence signal, we tried to better characterize the punctate fluorescence so that a more selective filter set could be designed. We began by analyzing the fluorescence spectra of growth medium (Dulbecco's modified Eagle medium [DMEM] powder; Life Technologies, Gaithersburg, MD, USA) (Catalog No. 13000-021, phenol red-free, supplemented with 25 mM HEPES, pH 7.3, 10% horse serum and 5% fetal calf serum) and a PC12 cell suspension in growth medium using a Hitachi F2000 fluorescence spectrophotometer (Hitachi Instruments, Danbury, CT, USA). Both the suspension and the growth medium had excitation and emission maxima of 450 nm and 530 nm, respectively, with significant emission extending out to 580 nm, yellow (Figure 1). These spectral properties were consistent with the properties of the intracellular punctate autofluorescence and raised the possibility that the cells were accumulating a fluorescent component from the medium into membrane compartments. The only constituent of DMEM with this fluorescence spectrum is riboflavin (4). When DMEM lacking riboflavin but containing serum was reanalyzed in the fluorescence spectrophotometer, the emission peak at 530 nm was not observed, indicating that riboflavin was the source of growth medium fluorescence. These data suggested that riboflavin

may be taken up by cells and concentrated within organelles known to contain flavinoids; these organelles that autofluoresce can be peroxisomes or mitochondria. In support of our data, a number of investigators have independently shown that flavins (FADH, FMN) and flavoproteins are responsible for yellow-green autofluorescence in living cells and in undefined organelles (1,2,11,12).

Standard fluorescein filter sets excite and emit light over a wide range of wavelengths that span the excitation and emission peaks of both S65T GFP and riboflavin. Since these two fluorescent species have excitation maxima separated by 40 nm and emission maxima separated by 20 nm (Figure 1), we have been able to design a fluorescence microscope filter set, more selective for visualizing GFP while avoiding peak excitation and emission wavelengths for riboflavin. Using a variety of excitation and emission filter combinations, we empirically determined that the most effective way to minimize the punctate autofluorescence while preserving the GFP signal was to excite cells with light around the S65T GFP excitation peak of 490 nm while avoiding excitation wavelengths around 450 nm. Ultimately, the following combination of filters was found to be most effective at reducing autofluorescence while preserving GFP fluorescence: 470–490-nm excitation filter (Omega Optical, Brattleboro, VT, USA), a 505-nm dichroic beamsplitter (Chroma Technology, Brattleboro, VT, USA) and a 510–532-nm emission filter (Omega Optical). Even with long exposure times (10 s), few autofluorescent vesicles could be seen with the modified filter set (Figure 2A) when compared with images taken by using a 415–445-nm excitation filter to accentuate the autofluorescent signal (Figure 2B). On the other hand, there was no observable difference in the intensity or distribution of the punctate autofluorescence between images acquired using the 415–445 nm excitation filter set and the standard fluorescein filter set. We hoped to reduce the autofluorescent signal further by growing BHK cells in riboflavin-free medium; however, the cultures did not proliferate under these conditions.

A second problem with viewing live cells bathed in growth medium was the appearance of a fluorescent yellow-green "haze" in the medium surrounding the cells obscuring the GFP signal. After several seconds of continuous illumination, the haze disappeared and the GFP signal improved. This apparent increase in GFP signal presumably was due to photobleaching of the riboflavin fluorescence. Since it took a few seconds of continuous illumination to reduce the haze, there was also some photobleaching of GFP fluorescence. To eliminate the yellow-green haze without unduly illuminating the cells, we expose the growth medium alone to ultraviolet (UV) light before viewing the cells—on the day cells are to be observed, 10 mL of the medium is placed in a 15-mL polypropylene conical tube and irradiated with short-wavelength UV light from a Foto/Prep® I UV light box (Fotodyne, Hartland, WI, USA) (four 15-W, 300-nm bulbs) for two min. The growth medium is removed and replaced by UV-treated medium just before viewing the cells. Alternatively, riboflavin-free DMEM containing animal sera can be used in place of UV-treated medium.

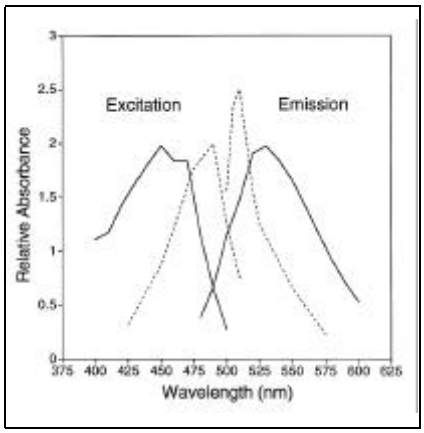

Figure 1. Comparison of the fluorescence spectra for DMEM and S65T GFP. DMEM (—) has an excitation and emission maxima of 450 nm and 530 nm, respectively. These peaks are not observed when riboflavin-free DMEM is analyzed in the same manner (data not shown). In contrast, the S65T GFP mutant (- - -) has an excitation and emission maxima of 490 nm and 510 nm, respectively (6). DMEM and GFP peak amplitudes are not directly comparable.

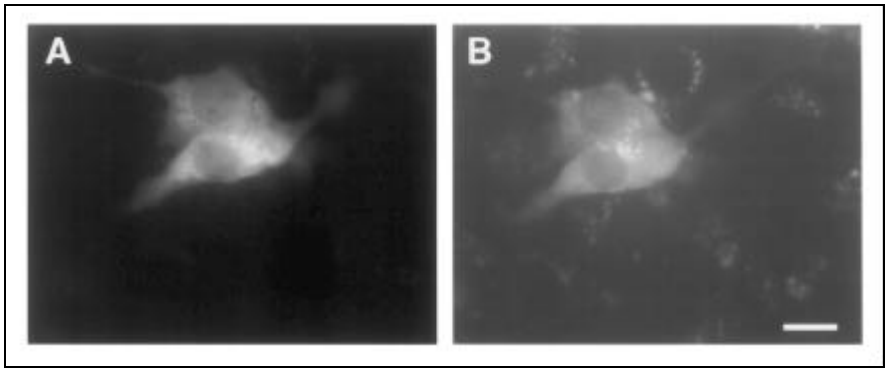

Figure 2. Optimized filter set used to image two live BHK cells transiently transfected with S65T GFP-rbKRP1 amidst a monolayer of untransfected cells. Cells photographed with (A) the optimized S65T GFP filter set (470–490-nm excitation filter, 505-nm dichroic beamsplitter, 510–532-nm emission filter) or (B) a filter set that primarily excites the yellow-green autofluorescence (415–445-nm excitation filter, 505-nm dichroic beamsplitter, 510–532-nm emission filter). Both exposures were for 10 s. Note that the punctate autofluorescence in both the transfected and the untransfected cells pictured in Panel B is greatly reduced when the optimized filter set is used (Panel A). There was virtually no difference between images acquired with the 415–445-nm excitation filter set and the standard fluorescein filter set. Method: BHK cells grown on 22 mm × 22 mm No. 1 glass coverslips were transfected with 2 mg of CsCl-purified plasmid DNA (pcDNA3 expression vector; Invitrogen, San Diego, CA, USA) using the calcium phosphate method (5) (30% efficiency). Live cells were observed roughly twenty-four hours after the transfection as follows: A well was created on a 24 mm × 60 mm No. 1 coverslip with silicone and filled with 100 µL warmed UV-treated medium (see text). A coverslip with adherent cells was inverted over the well and sealed with Vaseline™:lanolin:paraffin (1:1:1). Cells were viewed with the 63× 1.4 numerical aperture Plan-Apochromat objective of a Zeiss Axioskop microscope (Carl Zeiss, Thornwood, NY, USA) fitted with epifluorescence illumination from a mercury arc lamp. The entire microscope was encased in Plexiglas™ so that both the air and stage temperature around the microscope could be maintained at 37°C. Digital images were acquired with a cooled CCD camera and processed with Metamorph™ imaging software (Universal Imaging, West Chester, PA, USA). Cells maintained under these conditions remained viable for over an hour. Scale bar = 20 µm.

Although a number of investigators have successfully visualized GFP-fusion proteins in living cells with fluorescein filter sets, these data presented above suggest that there may be applications where weak yellow-green punctate autofluorescence can make it difficult to determine where GFP fluorescence is localized. Intracellular autofluorescence may plague many experiments using all forms of GFP, including the tyrosine 66 → histidine 66 (Y66H) blue GFP (7). This mutant has an excitation and emission maxima of 382 nm and 448 nm, respectively. When excited with 365-nm light, cells display an additional autofluorescence signal at 440 nm (blue) that is 50–100 times brighter than the yellow-green autofluorescence at 530 nm (1). This autofluorescence is presumably due to nicotinamide adenine dinucleotides and may pose even greater problems for investigators interested in imaging blue Y66H GFP fusion constructs in the future. To overcome all forms of autofluorescence, it may be useful to follow a strategy like the one that we have outlined above that involves designing a fluorescence filter set to maximally excite the molecule of interest while minimizing excitation of the autofluorescent species.

REFERENCES

1. **Aubin, J.E.** 1979. Autofluorescence of viable cultured mammalian cells. J. Histochem. Cytochem. *27*:36-43.
2. **Benson, R.C., R.A. Meyer, M.E. Zaruba and G.M. McKhann.** 1979. Cellular autofluorescence—is it due to flavins? J. Histochem. Cytochem. *27*:44-48.
3. **Chalfie, M., Y. Tu, G. Euskirchen, W.W. Ward and D.C. Prasher.** 1994. Green fluorescent protein as a marker for gene expression. Science *263*:802-805.
4. **Dawson, R.M.C, D.C. Elliot, W.H. Elliot and K.M. Jones.** 1986. Data for Biochemical Research, 3rd ed. Oxford University Press, New York.
5. **Graham, F.L. and A.J. van der Eb.** 1973. A new technique for the assay of infectivity of human adenovirus 5 DNA. Virology *52*:456-467.
6. **Heim, R., A.B. Cubitt and R.Y. Tsien.** 1995. Improved green fluorescence. Nature *373*:663-664.
7. **Heim, R., D.C. Prasher and R.Y. Tsien.** 1994. Wavelength mutations and posttranslational autooxidation of green fluorescent protein. Proc. Natl. Acad. Sci. USA *91*:12501-12504.
8. **Kaether, C. and H.H. Gerdes.** 1995. Visualization of protein transport along the secretory pathway using green fluorescent protein. FEBS Letters *369*:267-271.
9. **Kahana, J.A., B.J. Schnapp and P.A. Silver.** Kinetics of spindle pole body separation in budding yeast. Proc. Natl. Acad. Sci. USA *92*:9707-9711.
10. **Lim, C.R., Y. Kimata, M. Oka, K. Nomaguchi and K. Kohno.** 1995. Thermosensitivity of green fluorescent protein fluorescence utilized to reveal novel nuclear-like compartments in a mutant nucleoporin NSP1. J. Biochem. *118*:13-17.
11. **Mayeno, A.N., K.J. Hamann and G.J. Gleich.** 1992. Granule-associated flavin adenine dinucleotide (FAD) is responsible for

eosinophil autofluorescence. J. Leukoc. Biol. *51*:172-175.
12. **Nokubo, M., M. Ohta, K. Kitani and I. Z.-Nagy.** Identification of protein-bound riboflavin in rat hepatocyte plasma membrane as a source of autofluorescence. Biochim. Biophys. Acta *981*:303-308.
13. **Olson, K.R., J.R. McIntosh and J.B. Olmsted.** 1995. Analysis of MAP4 function in living cells using green fluorescent protein (GFP) chimeras. J. Cell Biol. *130*:639-650.
14. **Rizzuto, R., M. Brini, P. Pizzo, M. Murgia and T. Pozzan.** 1995. Chimeric green fluorescent protein as a tool for visualizing subcellular organelles in living cells. Curr. Biol. *5*:635-642.

The authors would like to thank Elena Porro for producing the S65T GFP-rbKRP1 construct, Roger Tsien for providing the S65T GFP mutant and Charlotte Vines for performing the growth studies in riboflavin-free medium. This work was supported by grants from The Council for Tobacco Research and from the NIH NS26846 to B.J.S. Address correspondence to Bruce J. Schnapp, Department of Cell Biology, Harvard Medical School, Building C, Room 633, 240 Longwood Avenue, Boston, MA 02115, USA. Internet schnapp@warren.med.harvard.edu

Received 14 November 1995; accepted 29 January 1996.

Mark J. Zylka and Bruce J. Schnapp
Harvard Medical School
Boston, MA, USA

Streamlined Protocol for Polytene Chromosome In Situ Hybridization

BioTechniques 21:226-230 (August 1996)

The ability to localize a gene sequence by polytene chromosome in situ hybridization (PISH) has long been a quintessential feature of *Drosophila* molecular genetics. Fittingly, numerous investigators have sought to optimize PISH, and a search of the FlyBase literature database (3) uncovers dozens of articles describing modifications of the technique. The end result of these efforts is several useful protocols that produce excellent results, and these should be consulted by anyone attempting PISH for the first time (1,2,5–9,11). However, I have found that these procedures contain extraneous or protracted steps that can be avoided while still producing excellent results. In this report, I detail a streamlined protocol (Table 1) that gives results that should satisfy the demands of nearly every investigator (Figure 1). Items that I do not discuss, such as squashing and probe labeling, are covered in the references noted above. The remainder of this article presents additional observations that may be of assistance in carrying out the procedure.

Although nearly every protocol recommends it, I have found it unnecessary for the microscope slides or coverslips to be washed with ethanol or detergent or treated with acid before using them. Also, I have seen no differences in the final results by using any combination of untreated or gelatin-coated (subbed) slides and untreated or silanized coverslips. These choices have more effect on the ease with which the chromosomes can be spread than anything else. The chromosomes essentially always stick to the slide no matter which combination is used. I prefer to use Superfrost®/Plus slides (Fisher Scientific, Pittsburgh, PA, USA) and untreated coverslips.

To make the chromosome preparations, I dissect and squash the larvae directly in 45% acetic acid; no additional fixatives are necessary. Thumb squashing works well if a small number of squashes are to be prepared; for larger endeavors, the method of Hepperle (4) provides an inexpensive solution to thumb fatigue.

While several reports have described using ethanol baths chilled to -70°C to dehydrate the frozen squash prepara-

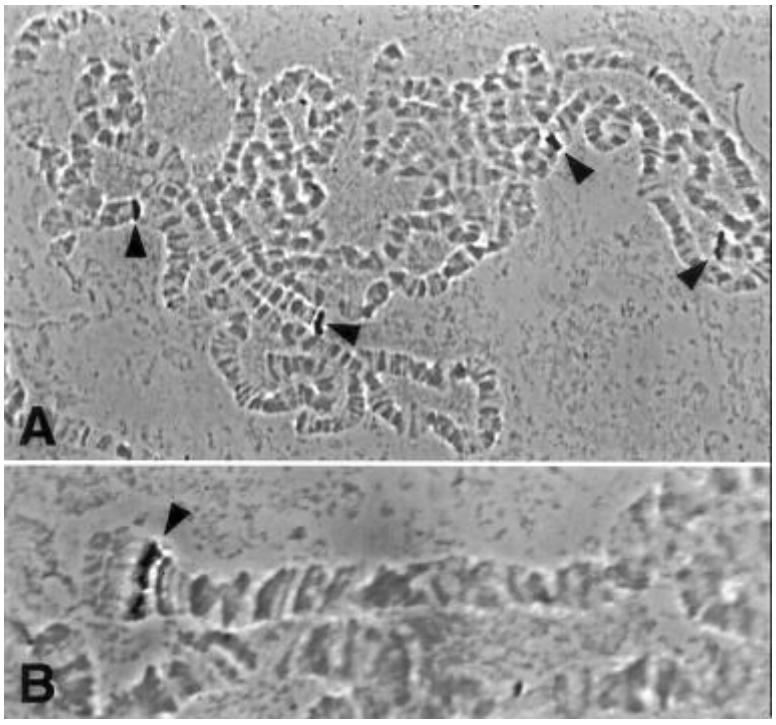

Figure 1. PISH used to localize the positions of transgenic P elements introduced into the genome by germ-line transformation. The digoxigenin-labeled probe specifically identifies the transgene. Arrowheads note the hybridization signal. For these photographs, the chromosomes were left unstained, and the plane of focus was centered on the hybridization signal. Orcein-stained chromosomes in the plane of focus would show significantly clearer detail. (A) Two nuclei, each showing signal at the two sites of transgene integration (polytene positions 21B and 42A). (B) A high magnification view of a different nucleus showing the signal at 21B.